

# Pressure dependence of melting temperatures in branched polyethylene up to 2 GPa

S. Saeki<sup>a,\*</sup>, S. Takei<sup>a</sup>, Y. Ookubo<sup>a</sup>, M. Tsubokawa<sup>a</sup>, T. Yamaguchi<sup>a</sup> and T. Kikegawa<sup>b</sup>

<sup>a</sup>Department of Materials Science and Engineering, Fukui University, Fukui 910, Japan

<sup>b</sup>National Laboratory for High Energy Physics, Tsukuba 305, Japan

(Received 7 April 1997; revised 8 August 1997; accepted 26 August 1997)

The melting temperatures ( $T_m$ ) of branched polyethylene (B-PE) have been measured over the pressure range up to 2 GPa by use of a high-pressure X-ray diffraction apparatus. The  $T_m$ - $P$  curve for B-PE is expressed as  $(T_m/T_{m,0})^c = (P + P_0)/a$  where  $T_{m,0}$  is the  $T_m$  at atmospheric pressure,  $c = 4.788$ ,  $P_0 = 280.2$  MPa and  $a = P_0 + 0.1$  MPa. The  $T_m$  of B-PE increases with increasing pressure monotonically, and  $T_m = 310^\circ\text{C}$  at 2 GPa. The X-ray diffraction peaks corresponding to the spacing  $d = 3.84$  Å for the (110) lattice plane of the orthorhombic B-PE crystal do not change with increasing temperature below 1.85 GPa but  $d$  values for the (200) lattice plane increase with increasing temperature. The thermal properties of a B-PE melt crystallized at various high pressures above 1.0 GPa have been measured at atmospheric pressure, and four endothermic peaks are observed for the sample melt crystallized at 800 MPa. The entropies of fusion  $\Delta S_F$  of B-PE and linear polyethylene (L-PE) at pressures up to 200 MPa have been determined based on the Clausius–Clapeyron equation and  $P$ - $V$ - $T$  data by O. Olabisi and R. Simha (*Macromolecules*, 1975, **8**, 206), and  $\Delta S_F$  for B-PE is much smaller than for L-PE. © 1998 Elsevier Science Ltd. All rights reserved.

(Keywords: melting temperature; branched polyethylene; high pressure)

## INTRODUCTION

It is well known that linear polyethylene (L-PE) forms an extended-chain crystal with a hexagonal structure at elevated pressures  $P > 330$  MPa, while below this pressure the crystal takes the form of a folded chain crystal with orthorhombic structure<sup>1,2</sup>. Recently, impressive work on the crystallization phenomena of linear polyethylene under high pressure has been carried out by Hikosaka *et al.*<sup>3</sup> and Rastogi *et al.*<sup>4</sup>, who found experimentally that the hexagonal phase is a metastable transient phase and exists even in the orthorhombic phase region in the phase diagram, and crystallization starts from the transient hexagonal structure and ends in the stable orthorhombic structure. Other impressive work in polymer crystallization is on pressure-induced crystallization and amorphization carried out by Rastogi *et al.*<sup>5</sup> for poly(4-methyl-1-pentene) where the melting temperature ( $T_m$ )-pressure ( $P$ ) curve displays a maximum point and amorphization occurs at high pressure at room temperature. Although most of the  $T_m$ - $P$  curves for crystalline polymers are convex upwards against pressure in the vicinity of 1 atm, so far no maximum point in the  $T_m$ - $P$  curve has been reported except for poly(4-methyl-1-pentene). The  $T_m$ - $P$  curves for crystalline polymers have been studied by Bassett and Turner<sup>6</sup>, Takamizawa *et al.*<sup>7</sup>, Yasuniwa *et al.*<sup>8</sup> and Hikosaka *et al.*<sup>9</sup> for linear polyethylene, and Nakafuku<sup>10,11</sup> and Nakafuku and Miyaki<sup>12</sup> for branched polyethylene, polypropylene and poly(1-butene). In a previous paper<sup>13</sup> we estimated the melting point maximum in the  $T_m$ - $P$  curve in branched polyethylene (B-PE) based on  $P$ - $V$ - $T$  data<sup>14</sup>. According to the Clausius–Clapeyron equation, the density of the liquid phase at the maximum  $T_m$  is the same as that of the solid or crystalline

phases. The main purpose of this work is to examine whether the  $T_m$  maximum is observed in B-PE by the measurement of  $T_m$  at high pressures above 2 GPa by using a high-pressure X-ray diffraction apparatus. We also investigated the existence of the high-pressure hexagonal phase in B-PE, the thermal properties of a B-PE melt crystallized under various pressures at atmospheric pressure, and the pressure dependence of the entropies of fusion of B-PE and L-PE.

## EXPERIMENTAL

The low-density branched polyethylenes used in this work are a Sowa Science Corp. sample (SSC-0.92;  $0.92\text{ cm}^3\text{ g}^{-1}$ ) and the NBS standard sample 1476 (NBS-0.9312;  $0.9312\text{ cm}^3\text{ g}^{-1}$  at  $23^\circ\text{C}$ ). The high-pressure X-ray diffraction apparatus used is the MAX80(AR-NE5C) instrument at the National Laboratory for High Energy Physics in Tsukuba, Japan. The MAX80(AR-NE5C) comprises a high-pressure apparatus with a cubic-type anvil and a maximum pressure of 6 GPa and a maximum temperature of  $2000^\circ\text{C}$ , and possesses a channel with an energy range 20–140 keV. The B-PE sample with a diameter of 4 mm and a thickness of 1.3 mm is placed in a sample vessel made of boron nitride (BN), which is covered by a gasket made of a boron–epoxy resin compound. The temperature of the sample is monitored by means of a chromel–alumel thermocouple and the sample pressure by the lattice constant of an NaCl crystal in the vessel based on NaCl  $P$ - $V$ - $T$  data<sup>15</sup>. In the energy-disperse X-ray diffractometer, the relationship between energy  $E$  (keV) and the distance between the lattice planes ( $d$  value) is given by  $E = 6.20/(d \sin \theta)$  where  $\theta$  is the angle of the incident beam; an angle of  $4.00^\circ$  is used in this work. The thermal

\*To whom correspondence should be addressed

properties of B-PE have been measured by use of a differential scanning calorimeter (Perkin-Elmer DSC7) with a heating rate of  $20^\circ\text{C min}^{-1}$ .

## RESULTS

Typical data obtained from the energy-dispersive X-ray diffractometer for the B-PE sample SSC-0.92 is shown in *Figure 1*. The X-ray diffraction measurements have been carried out over the range 0.7–1.9 GPa. The X-ray diffraction peak patterns for B-PE under constant pressure over the temperature range  $(T_m - 10^\circ\text{C}) < T < T_m$  are the same as that at room temperature, and no trace of new peaks for the high-pressure or hexagonal phase, as found for L-PE, is observed over the pressure range 0.7–1.9 GPa. No trace was also found of any new peaks in high-pressure d.t.a. up to 500 MPa<sup>10</sup>. However, X-ray diffraction peaks corresponding to the spacing  $d = 3.84 \text{ \AA}$  at 46.2 keV and the (110) lattice plane of the orthorhombic phase in B-PE (SSC-0.92) do not change with increasing temperature under 1.85 GPa, but  $d$  values at 51.5 keV for the (200) lattice plane increase with increasing temperature, as shown in *Figure 2*. The temperature at which the crystalline peak of B-PE corresponding to  $d = 4.10 \text{ \AA}$  for the (110) plane at atmospheric pressure disappears is determined as the melting

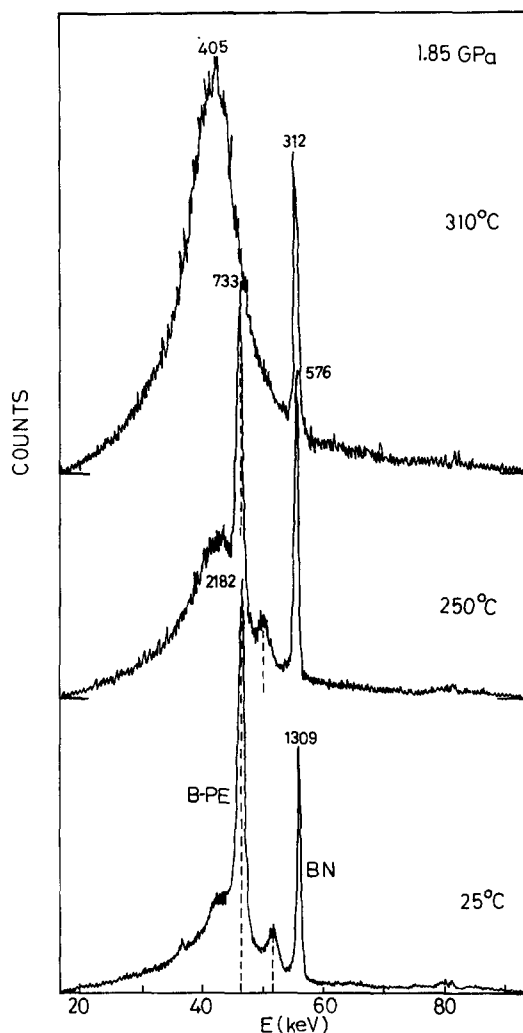


**Figure 1** Plot of X-ray intensity (counts) vs. energy (keV) for B-PE at a pressure of 1.85 GPa and at various temperatures. The values indicated are counts for each peak, and BN is boron nitride used as the pressure medium

temperature. The melting temperatures  $T_m$  are plotted against pressure in *Figure 3*, where the  $T_m$ - $P$  curves for B-PE (SSC-0.92 and NBS-0.9312), determined by high-pressure d.t.a. by Nakafuku<sup>10</sup> over pressures up to 500 MPa, and the  $T_m$ - $P$  curves for L-PE obtained by Hikosaka<sup>9</sup> are also included. The effect of thermal degradation of the polymer has been examined by investigating the reproducibility of  $T_m$  after the measurement of  $T_m$  at high temperatures and pressures. The reproducibility of  $T_m$  for B-PE (SSC-0.92) at atmospheric pressure is obtained within experimental error, which suggests that the effect of thermal degradation is not so large in the X-ray diffraction experiment under high pressure. However, values of  $T_m$  at pressures of 1.81 GPa, 1.128 GPa and 0.764 GPa, corresponding to the second, third and fourth runs, respectively, in the X-ray experiment, are slightly lower than in the  $T_m$ - $P$  curve determined from data obtained at 1.85 GPa (first run) and data obtained from 0.1 to 500 MPa at which the effect of thermal degradation may be negligible small. There is no maximum point for B-PE (SSC-0.92) in this work over 2.0 GPa. The  $T_m$ - $P$  functions for B-PE (SSC-0.92 and NBS-0.9312) are determined based on the Simon equation<sup>16</sup>

$$(T_m/T_{m,0})^c = (P + P_0)/a \quad (1)$$

where  $T_{m,0}$  is  $T_m$  at atmospheric pressure and  $a = (P_0 + 0.1) \text{ MPa}$ ,  $c$ ,  $P_0$  are constant and the values are listed in *Table 1* together with the values for L-PE. The curves in *Figure 3* are calculated by equation (1) using the constants in *Table 1*. The Simon equation (equation (1)) cannot predict the maximum point in the  $T_m$ - $P$  curve. The thermal properties of B-PE melt crystallized at various pressures have been measured at atmospheric pressure. Typical data indicating multiple endothermic peaks in the d.s.c. measurements are shown in *Figure 4*, where samples have been compressed up to a certain pressure at room temperature, heated to about  $20$ – $30^\circ\text{C}$  above the  $T_m$ , maintained at this temperature for about 2 h in order to liquefy the sample, then cooled to about  $20$ – $30^\circ\text{C}$  below the  $T_m$ , maintained at this temperature for about 2 h in order to crystallize the sample isothermally, and then cooled at room temperature. The  $P$ - $T$  processes are shown in *Figure 3*. Multiple peaks are observed for the first run of each fresh sample reproducibly, but a single peak appears during the second run.

## DISCUSSION

The pressure dependence of the melting point is usually discussed in terms of the Clausius–Clapeyron equation

$$dT_m/dP = (\Delta V_F/\Delta S_F) \quad (2)$$

where

$$\Delta V_F = V_{m,l} - V_{m,s} \quad (3)$$

and

$$\Delta S_F = S_{m,l} - S_{m,s} \quad (4)$$

**Table 1** The Simon constants for B-PE and L-PE

| Sample                  | $c$   | $P_0$<br>(MPa) |
|-------------------------|-------|----------------|
| B-PE (SSC-0.92)         | 4.788 | 280.2          |
| B-PE (NBS-0.9312)       | 4.774 | 232.3          |
| L-PE (H-O) <sup>a</sup> | 4.374 | 300.0          |
| L-PE (L-H) <sup>b</sup> | 3.139 | 453.3          |

<sup>a</sup>Hexagonal–orthorhombic transition line

<sup>b</sup>Liquid–hexagonal transition line

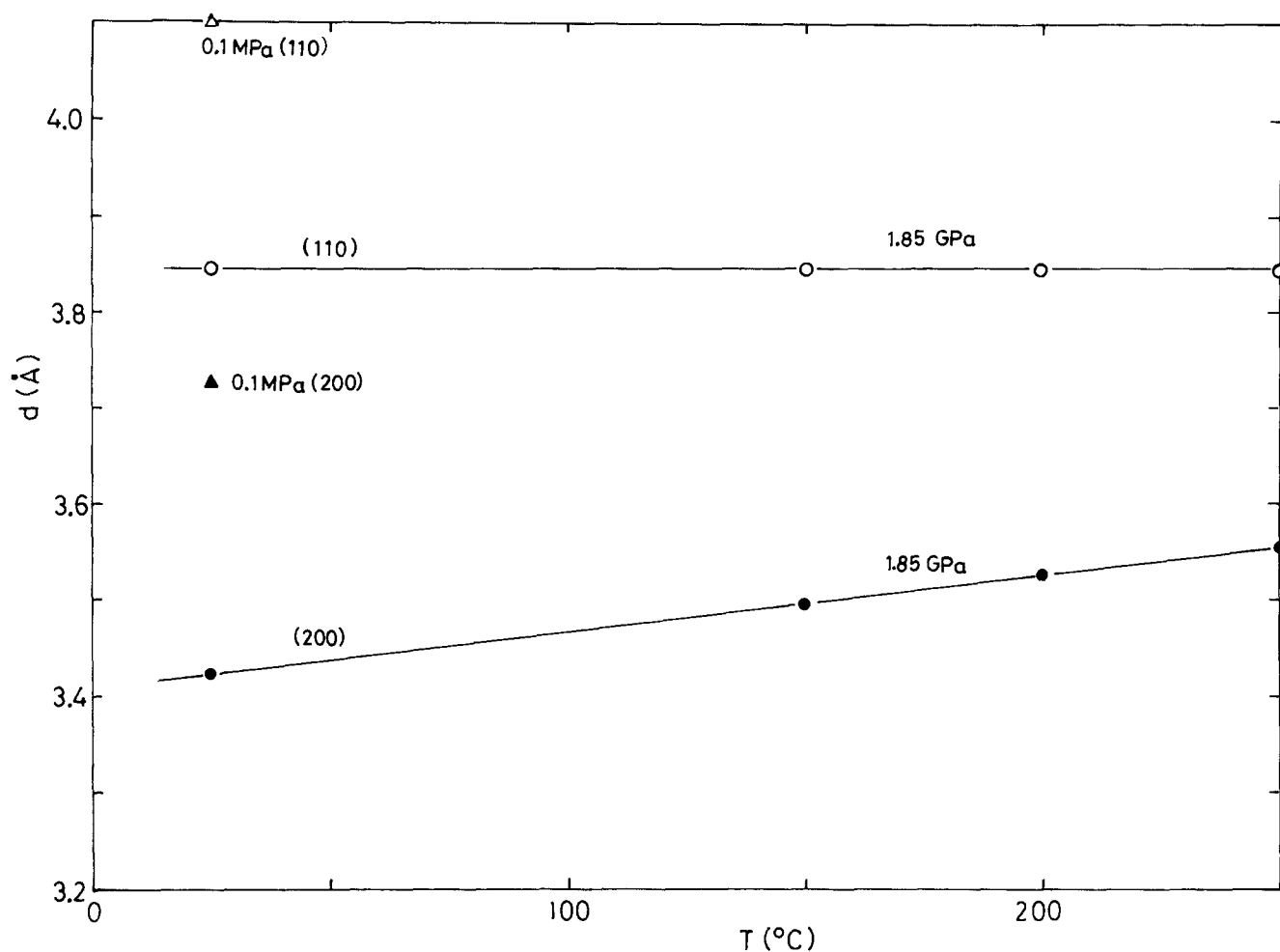


**Figure 2** Plot of the spacing of the lattice plane  $d$  for the (110) and (200) planes vs. temperature for B-PE at a pressure of 1.85 GPa. Data obtained at atmospheric pressure are also included

**Table 2** Thermodynamic quantities at the  $T_m$  for B-PE (NBS-0.9316) and L-PE

| $P_m$<br>(MPa) | $T_m$<br>(°C) | $\Delta V_F^a$<br>( $\text{cm}^3 \text{mol}^{-1}$ ) | $\Delta S_F^a$<br>( $\text{J K}^{-1} \text{mol}^{-1}$ ) | $\Delta H_F^a$<br>( $\text{J mol}^{-1}$ ) | $P_m \Delta V_F^a$<br>( $\text{J mol}^{-1}$ ) | $\Delta U_F^a$<br>( $\text{J mol}^{-1}$ ) |
|----------------|---------------|-----------------------------------------------------|---------------------------------------------------------|-------------------------------------------|-----------------------------------------------|-------------------------------------------|
| B-PE           |               |                                                     |                                                         |                                           |                                               |                                           |
| 0.1            | 116.6         | 1.627                                               | 4.632                                                   | 1805                                      | 0.1627                                        | 1805                                      |
| 50             | 131.7         | 1.262                                               | 4.191                                                   | 1697                                      | 63.1                                          | 1634                                      |
| 100            | 145.7         | 0.9537                                              | 3.603                                                   | 1509                                      | 95.37                                         | 1414                                      |
| 150            | 157.7         | 0.6732                                              | 2.841                                                   | 1224                                      | 100.9                                         | 1123                                      |
| 200            | 170.7         | 0.4488                                              | 2.087                                                   | 926                                       | 89.76                                         | 836                                       |
| L-PE           |               |                                                     |                                                         |                                           |                                               |                                           |
| 0.1            | 137.5         | 4.039                                               | 13.99                                                   | 5745                                      | 0.4039                                        | 5744                                      |
| 50             | 151.4         | 3.787                                               | 14.09                                                   | 5981                                      | 189.4                                         | 5791                                      |
| 100            | 164.4         | 3.646                                               | 14.47                                                   | 5966                                      | 364.6                                         | 5966                                      |
| 150            | 176.6         | 3.338                                               | 14.05                                                   | 6319                                      | 500.7                                         | 5818                                      |
| 200            | 188.2         | 3.057                                               | 13.59                                                   | 6269                                      | 611.4                                         | 5657                                      |

<sup>a</sup>The molecular (mol) unit is  $\text{CH}_2\text{CH}_2$ , equal to  $28.05 \text{ g mol}^{-1}$

where the suffix l denotes the liquid state and s the solid state at the melting point. The value of  $dT_m/dP$  for B-PE (NBS-0.9312) is obtained from equation (1),  $\Delta V_F$  is estimated based on  $P$ - $V$ - $T$  data<sup>14</sup> for B-PE (NBS-0.9312) over a temperature range including  $T_m$ , and then  $\Delta S_F$  is calculated by equation (2). The values of  $\Delta V_F$  and  $\Delta S_F$  for B-PE (NBS-0.9312) in this work and for L-PE are plotted against pressure in Figure 5, where both  $\Delta V_F$  and  $\Delta S_F$  for B-

PE are much smaller than those for L-PE. Although the Gibbs free energy change  $\Delta G_F$  at the melting point is zero, the internal energy change  $\Delta U_F$  is not zero at melting and is estimated by the relationship  $\Delta U_F = T_m \Delta S_F - P_m \Delta V_F$ . These values are given in Table 2 where it is shown that  $\Delta U_F$  for L-PE is almost constant at pressures over 200 MPa, while  $\Delta U_F$  for B-PE decreases with increasing pressure. The contribution of  $P_m \Delta V_F$ , which is the work due to volume

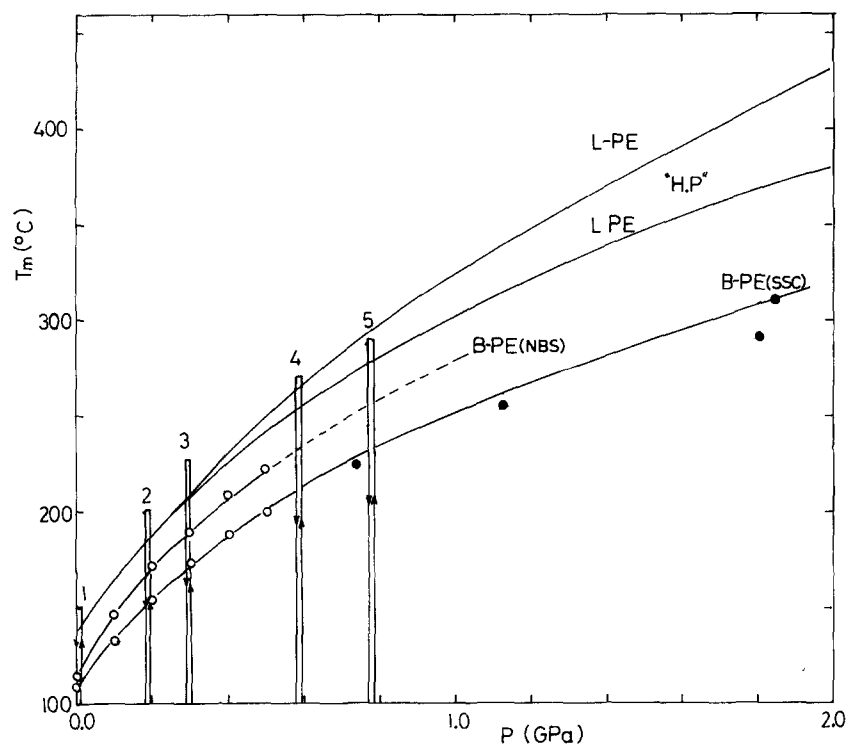


**Figure 3** The  $T_m$  vs.  $P$  phase diagram for B-PE. Empty circles, obtained by high-pressure differential thermal analysis by Nakafuku<sup>10</sup> up to 500 MPa; filled circles, determined by the high-pressure X-ray diffraction apparatus used in this work. The  $T_m$ - $P$  phase diagram for L-PE is also included. H.P. denotes the high-pressure hexagonal phase. The numbers indicated are the  $P$ - $T$  processes for the B-PE samples melt crystallized under pressure, which correspond to those in Figure 4

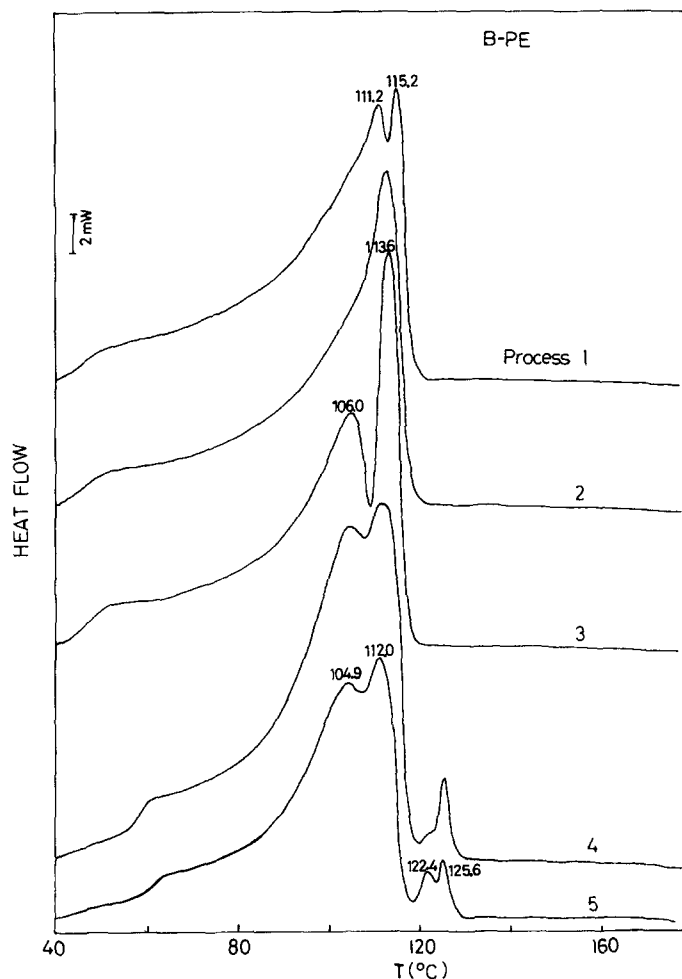


**Figure 4** Heat flow vs.  $T$  ( $^{\circ}\text{C}$ ) plot (first run) measured at atmospheric pressure for B-PE (SSC-0.92) melt crystallized by the various processes indicated in Figure 3

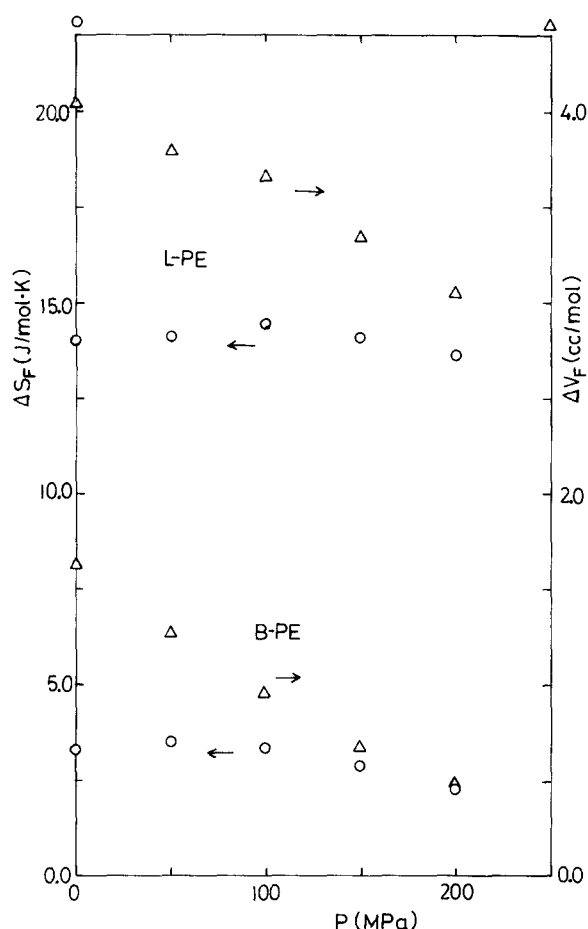


Figure 5 The entropy and volume of fusion against pressure for B-PE (NBS-0.9312) and L-PE calculated from  $P$ - $V$ - $T$  data and equation (1)

expansion at melting, to  $\Delta U_F$  is about 10% at higher pressures,  $P > 100$  MPa, but is negligible at atmospheric pressure.

It is interesting to point out that the  $T_m$ - $P$  functions for the two B-PE samples, with  $c = 4.788$  in equation (1) for SSC-0.92 and  $c = 4.774$  for NBS-0.9312, and the hexagonal-orthorhombic transition curve with  $c = 4.374$  for L-PE are almost the same. This also indicates that the  $T_m$ - $P$  curve for B-PE corresponds to the liquid-orthorhombic curve and therefore the liquid-hexagonal curve or the hexagonal phase itself does not exist in B-PE. It is important to discuss the reason why the hexagonal phase does not exist in B-PE. It is estimated from the  $P$ - $V$ - $T$  data<sup>14</sup> for B-PE and L-PE above 200 MPa that the specific volume at the melting point in the liquid state  $V_{m,l} = 1.121 \text{ cm}^3 \text{ g}^{-1}$ , and in the solid state  $V_{m,s} = 1.120 \text{ cm}^3 \text{ g}^{-1}$  for B-PE, while  $V_{m,l} = 1.129 \text{ cm}^3 \text{ g}^{-1}$  and  $V_{m,s} = 1.039 \text{ cm}^3 \text{ g}^{-1}$  for L-PE at 300 MPa. During the process of crystallization of L-PE by decreasing the temperature from  $T$  to  $T_m$  at a constant pressure such as 300 MPa, a large volume shrinkage  $\Delta V_c < 0$  occurs at crystallization and the polymer passes through various densities from low (liquid) to high (crystalline), and there is the possibility of attaining a new metastable phase during the change in density. On the

other hand, in the case of B-PE, the density change is negligibly small or  $\Delta V_c \approx 0$  because of the low density of crystalline B-PE due to the branched chain, and there is no chance of attaining a new metastable phase. In the case of poly(4-methyl-1-pentene), a new high-pressure phase (hexagonal phase) appears in the region of  $dT_m/dP < 0$ , where an expansion of the volume  $\Delta V_c > 0$  occurs at crystallization. It is speculated that the high-pressure phase appears when the volume change at crystallization under high pressure is large enough to attain a new phase.

The multiple melting peaks observed in B-PE in this work are also reported in an annealed sample of B-PE<sup>17</sup> and polyethylene copolymer with ethyl branches<sup>18</sup>. A higher melting peak appears in the sample melt crystallized at 800 MPa, which may be due to selected molecules consisting of linear parts and forming thick lamellae in B-PE.

## CONCLUSIONS

It has been found in this work that there is no maximum point in the  $T_m$ - $P$  curves for B-PE up to 2 GPa and there is no sign of a high-pressure phase in B-PE, from both X-ray diffraction and differential thermal analysis under high pressure.

## ACKNOWLEDGEMENTS

The authors express their grateful thanks to Professor C. Nakafuku (Kochi University) for valuable data for the melting temperatures of B-PE measured by high-pressure d.t.a.

## REFERENCES

1. Wunderlich, B. and Melillo, L., *Makromol. Chem.*, 1968, **118**, 250.
2. Bassett, S., Block, S. and Piermarini, G. J., *J. Appl. Phys.*, 1974, **45**, 4146.
3. Hikosaka, M., Rastogi, S., Keller, A. and Kawabata, H., *J. Macromol. Sci. Phys.*, 1992, **B31**(1), 87.
4. Rastogi, S., Hikosaka, M., Kawabata, H. and Keller, A., *Makromol. Chem., Macromol. Symp.*, 1991, **48/49**, 103.
5. Rastogi, S., Newman, M. and Keller, A., *J. Polym. Sci. Phys. Ed.*, 1993, **31**, 125.
6. Bassett, D. C. and Turner, B., *Philos. Mag.*, 1974, **29**, 925.
7. Takamizawa, K., Ohno, A. and Urabe, Y., *Polym. J.*, 1975, **7**, 342.
8. Yasuniwa, M., Enoshita, R. and Takemura, T., *Jpn. J. Appl. Phys.*, 1976, **15**, 1421.
9. Hikosaka, M., Minomura, S. and Seto, T., *Jpn. J. Appl. Phys.*, 1980, **19**, 1763.
10. Nakafuku, C., personal communication, 1993, 1997.
11. Nakafuku, C., *Polymer*, 1981, **22**, 1673.
12. Nakafuku, C. and Miyaki, T., *Polymer*, 1983, **24**, 141.
13. Saeki, S., Tsubokawa, M., Yamanaka, J. and Yamaguchi, T., *Polymer*, 1992, **33**, 577.
14. Olabisi, O. and Simha, R., *Macromolecules*, 1975, **8**, 206.
15. Decker, D. L., *J. Appl. Phys.*, 1971, **42**, 3239.
16. Simon, F. E. and Glatzel, G., *Anorg. Allg. Chem.*, 1929, **178**, 309.
17. Magill, J. H. and Peddada, S., *J. Polym. Sci. Polym. Phys. Ed.*, 1979, **17**, 1947.
18. Bassett, D. C., *Developments in Crystalline Polymers I*. Applied Science Publishers, 1982.